Letters

Simplified Analytical Modeling of Reflected Wave Transients in Cable-Connected VSI-Based Motor Drives With Output Reactor

Abdul Basit Mirza[®], Graduate Student Member, IEEE, Sama Salehi Vala[®], Graduate Student Member, IEEE, Kushan Choksi[®], Graduate Student Member, IEEE, and Fang Luo[®], Senior Member, IEEE

Abstract—This letter proposes a simplified lumped analytical model to investigate reflected wave phenomenon (RWP) in a twolevel voltage source inverter-based motor drive with an output reactor. RWP causes motor side overvoltage and drive side overcurrent. The output reactor at the drive side is a preferred RWP mitigation approach for its simplicity. However, existing RWP modeling approaches, for reactor design purposes, rely on complex cable and motor circuit models, requiring time-consuming simulations or are oversimplified, neglecting motor impedance and drive's output slew rate dv/dt. To address this, the proposed model incorporates a condensed motor model and a ramp edge source for the drive output. It is solved to obtain closed-form expressions for estimating the slew rate of overvoltage and overcurrent transients and their respective peak values. Finally, the derived expressions are validated through double pulse tests on a silicon carbide-based hardware prototype for different cable lengths and reactor values.

Index Terms—Drive side overcurrent, motor side overvoltage, output reactor, ramp edge, reflected wave phenomenon (RWP), silicon carbide (SiC), vector fitting.

I. INTRODUCTION

HE emergence of fast switching power semiconductor devices, such as wide bandgap, brings the concern of exacerbation of reflected wave phenomenon (RWP) in cable-connected motors powered by two-level (2L) voltage source inverter (VSI)-based motor drives [1], [2], [3]. RWP transients refers to the drive side overcurrent and motor side overvoltage, leading to decreased drive performance and accelerated motor winding insulation degradation. The extent of RWP in VSI-based drives depends on drive's output dv/dt, cable-motor differential mode (DM) impedance and pulse application timing [1].

For RWP mitigation, the output reactor or L filter at the drive output, owing to its simplicity, is widely employed for

Manuscript received 12 May 2024; revised 13 June 2024; accepted 29 June 2024. Date of publication 3 July 2024; date of current version 4 September 2024. This work was supported in part by Air Force Research Laboratory under Grant RSC23032 and Grant FA8650-19-D-2905 and in part by National Science Foundation through NSF under Grant 1846917. (Corresponding author: Abdul Rasit Mirza)

The authors are with the Department of Electrical and Computer Engineering, Stony Brook University, Stony Brook, NY 11790 USA (e-mail: abdulbasit. mirza@stonybrook.edu; sama.salehivala@stonybrook.edu; choksi.kushan@stonybrook.edu; fang.luo@stonybrook.edu).

Color versions of one or more figures in this article are available at https://doi.org/10.1109/TPEL.2024.3422324.

Digital Object Identifier 10.1109/TPEL.2024.3422324

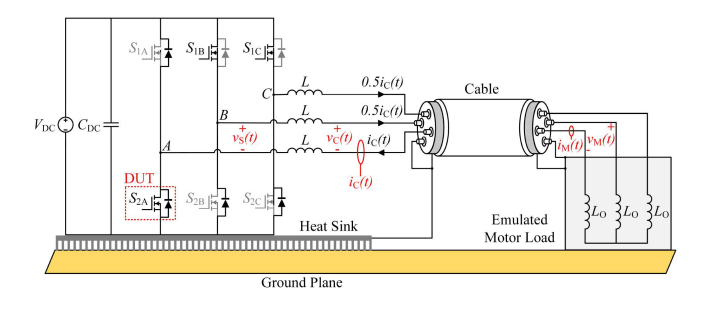
cable lengths up to 300 ft [4]. Generally, L is sized to keep its impedance at fundamental frequency within 3%-5% of the per-phase motor impedance to avoid significant voltage and power factor deterioration [5]. L lowers the reflected wave ringing frequency $f_{\rm RW}$, thereby reducing the slew rate of the RWP transients. It also helps reducing peak overvoltage, with the trend being almost proportional [1], [4]. However, as shown in this letter for short cable lengths, depending on system configuration, increasing L can increase peak overvoltage. Hence, it is crucial to analyze the impact of L on slew rate and peak overvoltage beforehand for reliable operation as mandated by standards, such as NEMA MG 1-2009 [6]. Likewise, it is essential to examine its impact on overcurrent transients, unexplored in the existing literature.

The existing approaches for predicting slew rate and peak values of RWP transients rely on complex cable and motor models, which either cannot be solved symbolically due to higher order characteristic function or require frequency domain analysis [3], [7], [8], [9]. Therefore, the user has to resort to using SPICE simulation or numerical analysis software.

Although simplified models with closed-form solutions have been proposed, they do not specifically address the L filter configuration, rely on conservative assumptions, and primarily focus on estimating peak overvoltage [6], [10], [11], [12]. In [10], a second-order approximation of the motor drive system with L and L||R filter is presented. Nonetheless, the approximation yields peak overvoltage to 2 per unit because the motor drive output is taken as an ideal step (infinite $\mathrm{d}v/\mathrm{d}t$) and the motor as an ideal open circuit. The same assumptions are also adopted in [6], and [11] focusing on drive-side LC filter design. Further, in [12], an expression for peak overvoltage, considering pulse rise time, is presented. Nevertheless, the expression requires the precise value of the reflection coefficient to be known.

This letter presents a simplified analytical model to investigate RWP in a cable-fed motor drive with output reactor. The model comprises lumped DM equivalent circuits of the reactor, cable, and motor connected to a pulse voltage source, representing the drive output. The impedance of the proposed model accurately models the total DM impedance $Z_{\rm DM}$ of the drive system up to the first antiresonance, the root cause of RWP in the L filter configuration [1], [4]. For the drive output, instead of a step source considered in [6], [10], and [11], which overestimates

0885-8993 © 2024 IEEE. Personal use is permitted, but republication/redistribution requires IEEE permission. See https://www.ieee.org/publications/rights/index.html for more information.



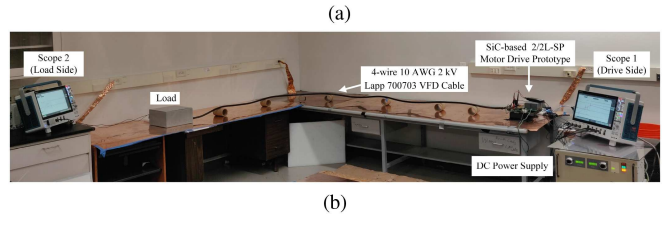


Fig. 1. 2L VSI cable-fed motor drive with output reactor. (a) Schematic. (b) Experimental setup.

RWP, a ramp edge source is utilized to account for the drive's output $\mathrm{d}v/\mathrm{d}t$. Further, closed-form expressions are obtained by simplifying the proposed model to estimate the slew rate of overvoltage and overcurrent transients and peak values. The expressions facilitate the reactor design and RWP analysis by eliminating characterization of complex cable and motor circuit models, followed by computationally expensive simulations. The model and derived expressions are validated through DPTs for two cable lengths and various reactor values on an 18 kVA SiC-based 2L VSI prototype interfaced with an emulated motor load through a bundled shielded cable.

II. LUMPED DM EQUIVALENT CIRCUIT MODELING

The RWP in drive systems with L filter is primarily attributed to the excitation of the first antiresonance at $f_{\rm RW}$ in $Z_{\rm DM}$ at each switching transition in each phase leg of the motor drive [1], [3]. The measurement procedure for $Z_{\rm DM}$ is discussed in [1], [2]. Fig. 1 depicts the schematic and experimental setup of cable-fed 2L VSI motor drive with an output reactor for the phase A bottom switch $S_{\rm 2~A}$ OFF \rightarrow ON switching transition with phase B and C clamped to dc link ($V_{\rm DC}$). To maintain consistency, this switching transition is considered throughout the letter. Further, the motor terminal (line–line) voltage and drive side output current, along with their respective peak overvoltage and overcurrent due to RWP, are denoted as $v_{\rm M}(t)$, $i_{\rm C}(t)$, $v_{\rm M(pk)}$ and $i_{\rm C(pk)}$, respectively.

The proposed equivalent DM circuit for Fig. 1(a) is presented in Fig. 2. $v_{\rm S}(t)$ represent the output pulse of the drive, with slope corresponding to ${\rm d}v/{\rm d}t$ of drain-source voltage of $S_{\rm 2\,A}$. The impedance $\tilde{Z}_{\rm DM}$ is intended to accurately model $f_{\rm RW}$ in $Z_{\rm DM}$. $1.5R_{\rm L}$ and $1.5\,L$ represent the net DM impedance of the output reactor. The cable is modeled as a single lumped RLC branch comprising $R_{\rm C}$, $L_{\rm C}$ and $C_{\rm C}$. The lumped approximation is valid as reactor value $L >> L_{\rm C}$ and dominates the RWP transient [10]. The DM impedance of the cable model is intended match to that of the actual cable $Z_{\rm DM,C}$ till its first antiresonance.

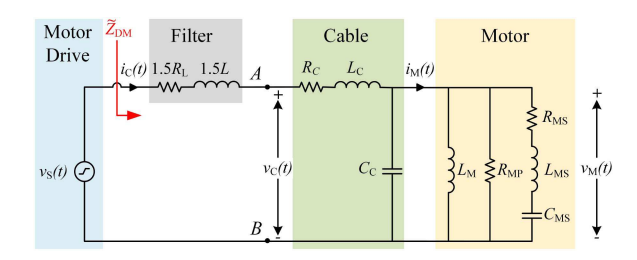


Fig. 2. Lumped DM equivalent circuit.

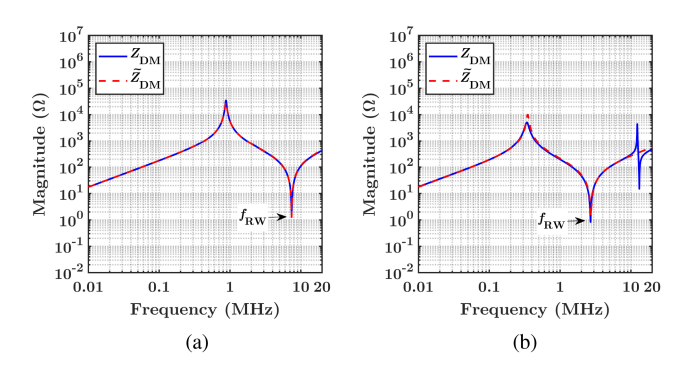


Fig. 3. Comparison of measured $Z_{\rm DM}$ and modeled $\tilde{Z}_{\rm DM}$ for two cable lengths with $L=2.35~\mu{\rm H}$. (a) 1 m. (b) 8 m.

Further, for the motor model, inspired from [7], $L_{\rm M}$ represents the DM inductance of the motor, which is 1.5 times the per phase inductance L_{ϕ} ($L_{\rm M}=1.5L_{\phi}$). The parallel branch containing $L_{\rm MS}$ and $C_{\rm MS}$ models the first antiresonance of the actual motor impedance $Z_{\rm DM,M}$. Lastly, $R_{\rm MP}$ and $R_{\rm MS}$ provides damping for the resonances.

The cable and motor models' component values can be determined through vector fitting measured $Z_{\rm DM,C}$ and $Z_{\rm DM,M}$ [13]. Fig. 3 compares $Z_{\rm DM}$ and $\tilde{Z}_{\rm DM}$ for the 1 and 8 m cable with $L=2.35~\mu{\rm H}$ for the experimental setup in Fig. 1(b). As can be seen, $\tilde{Z}_{\rm DM}$ matches with $Z_{\rm DM}$ accurately till $f_{\rm RW}$ and therefore can be used for modeling RWP transients.

III. DERIVATION OF CLOSED-FORM EXPRESSIONS

The proposed model in Fig. 2 can be solved to obtain expressions for $v_{\rm M}(t)$ and $i_{\rm C}(t)$, which can be used for estimating slew rates ${\rm d}v_{\rm M}(t)/{\rm d}t$ and ${\rm d}i_{\rm C}(t)/{\rm d}t$ and peak values $v_{\rm M(pk)}$ and $i_{\rm C(pk)}$. However, the underlying characteristic function is fifth-order, which cannot be solved symbolically. To address this, the proposed model can be further simplified based on the observation that the overvoltage and overcurrent transients are underdamped ($\zeta < 1$), with $v_{\rm M}(t)$ and $i_{\rm C}(t)$ reaching their peaks $v_{\rm M(pk)}$ and $i_{\rm C(pk)}$ at the onset of the transient where the value damping scaling term $e^{-\alpha t}\approx 1$. Therefore, $R_{\rm L}$, $R_{\rm C}$, $R_{\rm MP}$, and $R_{\rm MS}$ can be excluded, yielding the circuit in Fig. 4 with the following characteristic function in s-domain:

$$k_2 s^4 + k_1 s^2 + k_0 = 0. (1)$$

The coefficients k_2 , k_1 , and k_0 are given by

$$k_2 = (1.5L + L_{\rm C})L_{\rm M}L_{\rm MS}C_{\rm C}C_{\rm MS}$$
 (2)

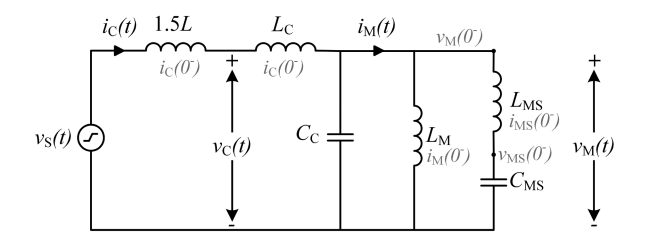


Fig. 4. Lumped DM equivalent circuit with damping ignored.

$$k_1 = L_{\rm M}(1.5L + L_{\rm C})(C_{\rm C} + C_{\rm MS}) + L_{\rm MS}C_{\rm MS}((1.5L + L_{\rm C}) + L_{\rm M})$$

$$k_0 = 1.5L + L_{\rm C} + L_{\rm M}.$$
(4)

With damping ignored $(s=j\omega)$, the circuit's response is oscillatory, characterized by pure complex roots $s_1=s_2^*$ and $s_3=s_4^*$. The magnitude of the roots are the angular frequencies $\omega_{\rm P1}$ and $\omega_{\rm P2}$ with $\omega_{\rm P1}<\omega_{\rm P2}$. $\omega_{\rm P1}$ is the first antiresonance $\omega_{\rm RW}=2\pi f_{\rm RW}$ responsible for RWP, while $\omega_{\rm P2}$ denotes the second antiresonance, which has minimal impact due to $\omega_{\rm P1}<<\omega_{\rm P2}$, caused by L. Therefore, $\omega_{\rm P1}=\omega_{\rm RW}$ becomes the dominant pole, governing the RWP transient [1]. The expressions for angular frequencies are

$$\omega_{\text{RW}} = \left| \sqrt{\frac{\sqrt{k_1^2 - 4k_2k_0} - k_1}}{2k_2} \right| \tag{5}$$

$$\omega_{P2} = \left| \sqrt{-\frac{\sqrt{k_1^2 - 4k_2k_0} + k_1}}{2k_2} \right|. \tag{6}$$

The RWP transient heavily depends on the slew rate of $v_{\rm S}(t)$ [1], [2], [3]. Therefore, a ramp edge with a rise time $T_{\rm R}$, corresponding to the drive's output ${\rm d}v/{\rm d}t$, is considered as follows:

$$v_{\rm S}(t) = \frac{V_{\rm DC}}{T_{\rm R}} \left(r(t) - r(t - T_{\rm R}) \right)$$
 (7)

where r(t) represents the unit ramp tu(t). The closed-form expressions for $v_{\rm M}(t)$ and $i_{\rm C}(t)$ can be obtained through s-domain analysis of Fig. 4 and taking inverse laplace.

$A. v_M(t)$

The expression for $v_{\rm M}(t)$ can be derived as

$$v_{\rm M}(t) = \frac{V_{\rm DC}L_{\rm M}}{T_{\rm R}(1.5L + L_{\rm C} + L_{\rm M})} (r(t) - r(t - T_{\rm R}))$$
$$+ v_{\rm AC}(t)u(t) + v_{\rm AC}(t - T_{\rm R})u(t - T_{\rm R}) \tag{8}$$

where $v_{\rm AC}(t)$ comprises sinusoidal terms, with angular frequency $\omega_{\rm RW}$, constituting to the overvoltage ringing transients

$$v_{\text{AC}}(t) = f(\mathbf{x})\sin(\omega_{\text{RW}}t) + g(\mathbf{x})\cos(\omega_{\text{RW}}t)$$
(9)
$$\mathbf{x} = [i_{\text{C}}(0^{-}), v_{\text{M}}(0^{-}), i_{\text{M}}(0^{-}), i_{\text{MS}}(0^{-}), v_{\text{MS}}(0^{-}), \omega_{\text{RW}}, \omega_{\text{P2}}, T_{\text{R}}].$$
(10)

The amplitudes f(x) and g(x) are given by

$$f(x) = \frac{v_0 - v_2 \omega_{\text{RW}}^2}{\omega_{\text{RW}}(\omega_{\text{P2}}^2 - \omega_{\text{RW}}^2)}$$
(11)

$$g(\mathbf{x}) = \frac{v_1 - v_3 \omega_{\text{RW}}^2}{(\omega_{\text{P2}}^2 - \omega_{\text{RW}}^2)}.$$
 (12)

The coefficients v_3 , v_2 , v_1 , and v_0 are given by

$$v_3 = v_{\mathsf{M}}(0^-) \tag{13}$$

$$v_2 = \frac{i_{\rm C}(0^-) - i_{\rm M}(0^-) - i_{\rm MS}(0^-)}{C_{\rm C}} - \frac{L_{\rm M}V_{\rm DC}}{T_{\rm R}(1.5L + L_{\rm C} + L_{\rm M})}$$
(14)

$$v_1 = \frac{C_{\rm C}v_{\rm M}(0^-) + C_{\rm MS}v_{\rm MS}(0^-)}{L_{\rm MS}C_{\rm C}C_{\rm MS}}$$
(15)

$$v_0 = \frac{i_{\rm C}(0^-) - i_{\rm M}(0^-)}{L_{\rm MS}C_{\rm C}C_{\rm MS}} - \frac{L_{\rm M}V_{\rm DC}(C_{\rm C} + C_{\rm MS})}{T_{\rm R}L_{\rm MS}C_{\rm C}C_{\rm MS}(1.5L + L_{\rm C} + L_{\rm M})}.$$
(16)

With damping, $v_{\rm AC}(t)$ in (8) decays over time. However, the purpose of (8) is to estimate ${\rm d}v_{\rm M}(t)/{\rm d}t$ and $v_{\rm M(pk)}$. The slew-rate, based on 10%–90% value criterion, is approximately the maximum slope of $v_{\rm AC}(t)$ at $v_{\rm AC}(t)=0$. Further, $v_{\rm M(pk)}$ is sum of the maximum value of $v_{\rm AC}(t)$ and steady state voltage. Through trigonometric simplification, following expressions can be obtained:

$$\frac{\mathrm{d}v_{\mathrm{M}}(t)}{\mathrm{d}t} \approx 2\omega_{\mathrm{RW}} \sin\left(\frac{T_{\mathrm{R}}}{2}\omega_{\mathrm{RW}}\right) \sqrt{f^{2}(\boldsymbol{x}) + g^{2}(\boldsymbol{x})} 10^{-9} \quad \text{(V/ns)}$$
(17)

$$\begin{split} v_{\rm M(pk)} &= \frac{V_{\rm DC}L_{\rm M}}{(1.5L + L_{\rm C} + L_{\rm M})} + \max\{v_{\rm AC}(t) - v_{\rm AC}(t - T_{\rm R})\} \\ &= \frac{V_{\rm DC}L_{\rm M}}{(1.5L + L_{\rm C} + L_{\rm M})} + 2\sin\left(\frac{T_{\rm R}}{2}\omega_{\rm RW}\right)\!\sqrt{f^2(x) + g^2(x)}. \end{split} \tag{18}$$

B. $i_C(t)$

The voltage $v_{\rm S}(t)-v_{\rm M}(t)$ across $1.5L+L_{\rm C}$ can be integrated to obtain expression for $i_{\rm C}(t)$ (19). Further algebraic manipulation of (19) yields the expression for $di_{\rm C}(t)/dt$, based on 10%–90% value criterion, and $i_{\rm C(pk)}$

$$i_{\rm C}(t) = \frac{1}{(1.5L + L_{\rm C})} \int_0^t (v_{\rm S}(\tau) - v_{\rm M}(\tau)) d\tau + i_{\rm C}(0^-)$$
(19)

$$\frac{\mathrm{d}i_{\mathrm{C}}(t)}{\mathrm{d}t} \approx 2\mathrm{sin}\left(\frac{T_{\mathrm{R}}}{2}\omega_{\mathrm{RW}}\right) \left[\frac{\sqrt{f^{2}(\boldsymbol{x}) + g^{2}(\boldsymbol{x})}}{(1.5L + L_{\mathrm{C}})}\right] 10^{-9} \quad \text{(A/ns)}$$
(20)

$$i_{\text{C(pk)}} = i_{\text{C}}(0^{-}) + 2\sin\left(\frac{T_{\text{R}}}{2}\omega_{\text{RW}}\right) \left[\frac{\sqrt{f^{2}(x) + g^{2}(x)}}{\omega_{\text{RW}}(1.5L + L_{\text{C}})}\right].$$
 (21)

C. Remarks

The sinusoidal scaling term $\sin(0.5T_{\rm R}\omega_{\rm RW})$ in the expressions for $v_{\rm M(pk)}$ and $i_{\rm C(pk)}$ provides valuable insight into RWP. If $T_{\rm R}=nT_{\rm RW}$, where n is a set of positive integers $(n=1,2,3,\ldots)$ and $T_{\rm RW}=2\pi/\omega_{\rm RW}$, the scaling term becomes zero and the RWP is ideally eliminated. Likewise, the expressions for ${\rm d}v_{\rm M}(t)/{\rm d}t$ and ${\rm d}i_{\rm C}(t)/{\rm d}t$ are applicable for $T_{\rm R}< T_{\rm RW}$. For $T_{\rm R}\geq T_{\rm RW}$, the slew rate solely depends on ratio of steady stage value and $T_{\rm R}$. This is also consistent with the analysis presented in [2].

Moreover, the initial current variables $i_C(0^-)$, $i_M(0^-)$ and $i_{MS}(0^-)$ only affect $v_{M(pk)}$ and $i_{C(pk)}$ when the prior RWP transient is not fully decayed. For instance, in Fig. 4, if the prior RWP transient is completely decayed, the voltage across C_C and C_{MS} is clamped, and no current flows through L_{MS} , resulting in $i_C(0^-)=i_M(0^-)$. Therefore, the influence of initial current values on v_0 and v_2 and subsequently on f(x) and g(x) is eliminated.

D. Extension to dv/dt Filters

The proposed lumped equivalent circuit model in Fig. 2 can be extended to dv/dt filters, which are broadly classified into LC and RLC types and encompass various variants [14]. These filters are essentially an extension of the output reactor configuration with an additional C (LC type) or RC (RLC type) branch to enhance RWP suppression [1].

For modeling these filters, the proposed lumped circuit model in Fig. 2 needs to be modified by adding the DM equivalent C branch for LC type, or R and C branch for RLC type $\mathrm{d}v/\mathrm{d}t$ filter across nodes A and B. The existing DM equivalent of the output reactor in Fig. 2 serves as the inductive L component of the filter.

However, the addition of R or RC branch in the proposed lumped circuit model raises concerns about a higher order characteristic function with a nongeneralized closed-form solution. Consequently, numerical analysis techniques can be used to obtain the solution of the characteristic function and subsequently estimate the slew rate and peak value of overvoltage and overcurrent transients for filter analysis and design purposes.

IV. EXPERIMENTAL VALIDATION

To verify the proposed model and derived expressions, DPTs are performed for the bottom device $S_{2\,\mathrm{A}}$ of phase A in Fig. 1 at 600 V and 32 A for two cable lengths (1 and 8 m) and five values of L (0, 0.075, 0.5, 2.35, and 5 μ H). The 0–5 μ H range for L is chosen to keep the maximum % impedance/inductance of L to within 3% of the per-phase value $L_{\phi}=(2/3)L_{\mathrm{M}}=183.41~\mu\mathrm{H}$ (see Table I). The top devices S_{1B} and S_{1C} of phases B and C are latched in the ON state, while the grayed-out devices are latched in the OFF state by giving a constant low logic to their gate drivers. The external ON and OFF gate resistances for $S_{2\,\mathrm{A}}$ are set to 2.5 and 0.47 Ω , respectively.

A MATLAB code is written to generate waveforms for $v_{\rm M}(t)$ and $i_{\rm C}(t)$ using (8) and (19) for the second turn-ON transient of $S_{\rm 2.A}$. The cable and load parameters are extracted using vector

TABLE I
EXTRACTED CABLE AND LOAD PARAMETERS

Parameter	Value	
	1 m	8 m
$L_{\rm C}$ (nH)	170.95	926.01
C _C (pF)	140.20	815.07
$L_{ m M}$ (μ H)	275.12	
$L_{ m MS}$ ($\mu m H$)	4.40	
C _{MS} (pF)	14.28	

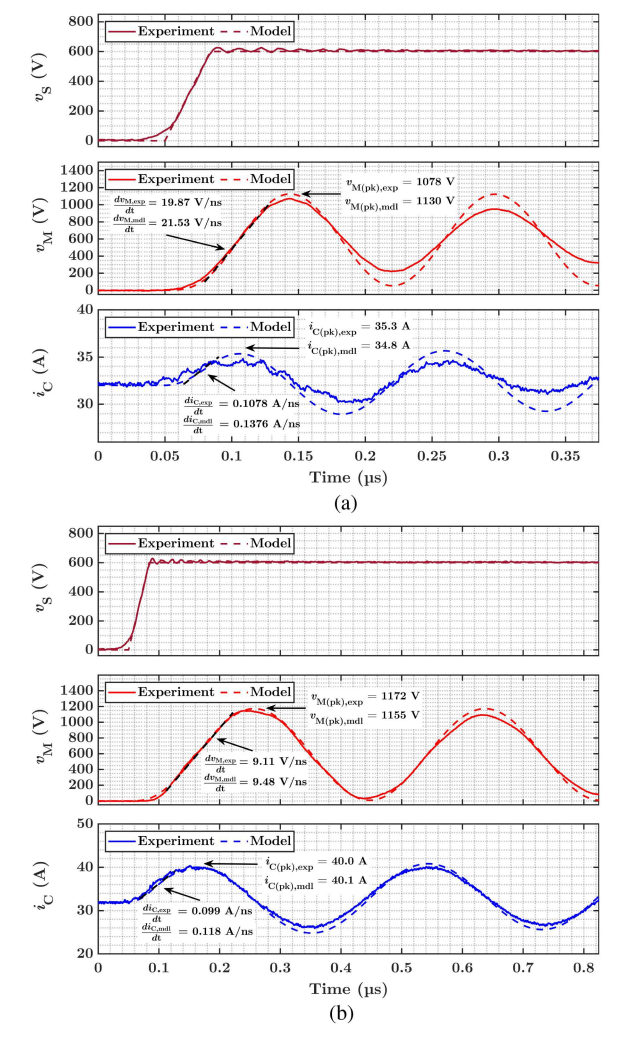


Fig. 5. Comparison of experimental and the proposed model-generated waveforms for $v_{\rm M}(t)$ and $i_{\rm C}(t)$ with $L=2.35~\mu{\rm H}$. (a) 1 m. (b) 8 m.

fitting (see Table I). The value of $T_{\rm R}$ for $v_{\rm S}(t)$ is extracted from the measured waveform.

For brevity, Fig. 5 compares the measured and model-generated waveforms for 1 and 8 m cable for $L=2.35~\mu{\rm H}.$ The rising trajectory of modeled $v_{\rm M}(t)$ and $i_{\rm C}(t)$ matches closely with the measured waveforms as the slew rate of $v_{\rm S}(t)$ is considered in the proposed circuit model. For 8 m cable, the slew rate and peak values of the modeled waveforms match accurately with the experimental results. However, for 1 m cable, the

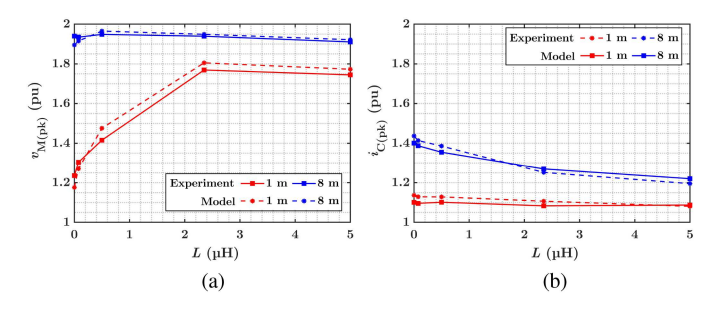


Fig. 6. Comparison of the variation of measured and calculated peak values with L. (a) $v_{M(pk)}$. (b) $i_{C(pk)}$.

model slightly overestimates these values. This overestimation is attributed to the lower settling time for 1 m than 8 m due to the lower value of $L_{\rm C}$ and $C_{\rm C}$, increasing the damping factor ζ [1]. As a result, the first peak for 1 m experiences slightly higher damping than 8 m. Nevertheless, the error in the measured and modeled peak values for 1 m cable is less than 5%.

Further, the variation of measured and calculated $v_{\rm M(pk)}$ and $i_{\rm C(pk)}$, using (18) and (21), with L, for both cable lengths is shown in Fig. 6. The values are plotted per unit with bases values as the steady stage voltage value $V_{\rm DC}L_{\rm M}/(1.5L+L_{\rm C}+L_{\rm M})$ for $v_{\rm M(pk)}$ and 32 A for $i_{\rm C(pk)}$. The predicted trend follows the measured, justifying the efficacy of the proposed model and derived expressions.

For $v_{\mathrm{M(pk)}}$, a dissimilar trend is observed with $v_{\mathrm{M(pk)}}$ rising with L for 1 m and falling slightly for 8 m. This trend implies that for short cable lengths, depending on the reactor, cable and motor load impedance interaction and the value of T_{R} , the addition of L can cause higher $v_{\mathrm{M(pk)}}$. Conversely, $i_{\mathrm{C(pk)}}$ exhibits a falling trend with L for both cable lengths.

V. CONCLUSION

A simplified lumped DM analytical circuit model, incorporating the output slew rate (dv/dt) of the motor drive, is proposed in this letter to simplify RWP investigation in cable-fed 2 L VSI-based motor drive systems with output reactor. The model is solved to obtain closed-form expressions that predict the transient trajectory and estimate the peak values for overvoltage and overcurrent. The effectiveness of the model and derived expressions is validated on hardware for short and long cable lengths and reactor values. Notably, a rising overvoltage pattern with increasing reactor value is observed for the short cable, which is captured by the model with accuracy. This trend suggests that increasing reactor value does not necessarily lower overvoltage, as suggested in the literature. Therefore, from a design perspective, the proposed model and derived expressions provide a more straightforward means

of analyzing the overvoltage and overcurrent transient trends beforehand.

ACKNOWLEDGMENT

The authors would like to acknowledge James Acquaviva, Center Director of the Advanced Energy Center (AERTC) at Stony Brook University, for providing support during hardware testing.

REFERENCES

- B. Narayanasamy, A. S. Sathyanarayanan, F. Luo, and C. Chen, "Reflected wave phenomenon in SiC motor drives: Consequences, boundaries, and mitigation," *IEEE Trans. Power Electron.*, vol. 35, no. 10, pp. 10629–10642, Oct. 2020.
- [2] W. Zhou, M. Diab, X. Yuan, and C. Wei, "Mitigation of motor overvoltage in SiC-Based drives using soft-switching voltage slew-rate (dv/dt) profiling," *IEEE Trans. Power Electron.*, vol. 37, no. 8, pp. 9612–9628, Aug. 2022.
- [3] S. Sundeep, J. Wang, A. Griffo, and F. Alvarez-Gonzalez, "Antiresonance phenomenon and peak voltage stress within PWM inverter fed stator winding," *IEEE Trans. Ind. Electron.*, vol. 68, no. 12, pp. 11826–11836, Dec. 2021.
- [4] H.-J. Kim, G.-H. Lee, C.-H. Jang, and J.-P. Lee, "Cost-effective design of an inverter output reactor in ASD applications," *IEEE Trans. Ind. Electron.*, vol. 48, no. 6, pp. 1128–1135, Dec. 2001.
- [5] Eaton, "Output filters and motor lead length," 2020. [Online]. Available: https://www.eaton.com/content/dam/eaton/products/industrialcontrolsdrives-automation-sensors/variable-frequency-drives/powerxl-dh1variable-frequency-drives/output-filters-and-motor-lead-lengthap040213en.pdf
- [6] H. Kim, A. Anurag, S. Acharya, and S. Bhattacharya, "Analytical study of SiC MOSFET based inverter output DV/DT mitigation and loss comparison with a passive DV/DT filter for high frequency motor drive applications," *IEEE Access*, vol. 9, pp. 15228–15238, 2021.
- [7] L. Wang, C. N.-M. Ho, F. Canales, and J. Jatskevich, "High-frequency modeling of the long-cable-fed induction motor drive system using TLM approach for predicting overvoltage transients," *IEEE Trans. Power Elec*tron., vol. 25, no. 10, pp. 2653–2664, Oct. 2010.
- [8] Y. Wu, K. Choksi, M. ul Hassan, and F. Luo, "An extendable and accurate high-frequency modelling of three-phase cable for prediction of reflected wave phenomenon," in *Proc. IEEE Appl. Power Electron. Conf. Expo.*, 2022, pp. 944–950.
- [9] N. Wang, C. Qian, Z. J. Wang, and Y. Kang, "An accurate analytical model for motor terminal overvoltage prediction and mitigation in SiC motor drives," in *Proc. IEEE Workshop Wide Bandgap Power Devices Appl. Asia*, 2021, pp. 504–509.
- [10] Z. Liu and G. L. Skibinski, "Method to reduce overvoltage on AC motor insulation from inverters with ultra-long cable," in *Proc. IEEE Int. Electric Machines Drives Conf.*, 2017, pp. 1–8.
- [11] J.-P. Strom, J. Korhonen, J. Tyster, and P. Silventoinen, "Active du/dt-new output-filtering approach for inverter-fed electric drives," *IEEE Trans. Ind. Electron.*, vol. 58, no. 9, pp. 3840–3847, Sep. 2011.
- [12] A. von Jouanne and P. Enjeti, "Design considerations for an inverter output filter to mitigate the effects of long motor leads in ASD applications," *IEEE Trans. Ind. Appl.*, vol. 33, no. 5, pp. 1138–1145, Sep./Oct. 1997.
- [13] G. Antonini, "SPICE equivalent circuits of frequency-domain responses," IEEE Trans. Electromagn. Compat., vol. 45, no. 3, pp. 502–512, Aug. 2003.
- [14] J. He, G. Y. Sizov, P. Zhang, and N. A. Demerdash, "A review of mitigation methods for overvoltage in long-cable-fed PWM AC drives," in *Proc. IEEE Energy Convers. Congr. Expo.*, 2011, pp. 2160–2166.